

Effects of V and Zn codoping on the microstructures and photocatalytic activities of nanocrystalline TiO₂ films

Fang Li^a, Ling-xiao Guan^b, Mei-li Dai^a, Ji-jun Feng^a, Ming-ming Yao^{a,*}

^aKey Laboratory of Chemical Sensing & Analysis in Universities of Shandong, School of Chemistry and Chemical Engineering, University of Jinan, Jinan 250022, China

^bSchool of Chemistry and Chemical Engineering, Ning Xia Teachers University, Guyuan 75600, China

Received 10 December 2012; received in revised form 6 February 2013; accepted 23 February 2013

Available online 4 March 2013

Abstract

To enhance the photocatalytic activity of TiO₂, V and Zn co-doped TiO₂ films were synthesized by the sol–gel method. The experimental results indicated that the films were composed of round-like nano-particles or aggregates. V and Zn codoping could not only obviously increase the specific surface area of TiO₂ but also result in the narrowed band gap of TiO₂ sample. The photocatalytic activities of the TiO₂ films were evaluated by the photocatalytic decomposition of organic dyes in aqueous solution. Compared with undoped TiO₂ film or single doped TiO₂ film, V and Zn co-doped TiO₂ film exhibited excellent photocatalytic activities under both UV light and visible light. The improvement mechanism by V and Zn codoping was also discussed.

© 2013 Elsevier Ltd and Techna Group S.r.l. All rights reserved.

Keywords: TiO₂ film; V and Zn codoping; Microstructure; Photocatalytic activity

1. Introduction

Wide band gap transition metal oxide semiconductor materials have attracted considerable research interest in the past few decades because of their unique properties. Among these heterogeneous semiconductors, TiO₂ is the most widely used photocatalytic material because of its strong oxidizing power, photo-stability, non-toxicity, chemical and biological inertness, as well as its low cost [1–3]. However, wide application of TiO₂-based photocatalytic technology has been restricted by three major factors [4]: (a) tedious operation to recover the powder catalyst; (b) low photocatalytic efficiency due to recombination of photogenerated electrons and holes; and (c) low visible light utilization efficiency due to the wide band gap of TiO₂ (3.2–3.4 eV). To overcome these drawbacks, many techniques were proposed to improve photocatalytic

activity of TiO₂, such as various preparations, composite semiconductors [5], metal or nonmetal doping [6,7], etc.

Metal ion doping is one of the most effective ways to enhance the photocatalytic activity of TiO₂. Compared with noble metals and lanthanide metals, modification of TiO₂ with transition metals provides a successful and cost effective alternative. Transition metal ions are doped into the TiO₂ lattice to modify its microstructures and electronic structures. Chang and Liu [8] reported that vanadium doped titanium dioxide films in the surface lattice could separate charge carriers and promote the photocatalytic activities of micrometer-sized TiO₂. Lu et al. [9] prepared an efficient photocatalyst Zn²⁺–TiO₂ by the sol–gel method. Experiment indicated that Zn²⁺-doping reduced the crystallite size of TiO₂ and the agglomeration of TiO₂ powder, thus displayed higher photocatalytic activity and regeneration ability than TiO₂. Although single metal doping can enhance the visible light response, single dopant has to be used in small quantity to avoid recombination of photogenerated electrons and holes. Therefore, the higher dye decomposition cannot be achieved by using

*Corresponding author. Tel.: +86 531 82765959;
fax: +86 531 82765969.

E-mail addresses: yaomm4364@sina.com, chm_lif@ujn.edu.cn
(M.-m. Yao).

single dopant with higher amount. Recently, a low concentration codoping of ions are reported to have higher photocatalytic activity than that of TiO_2 doped with single ions [10,11]. Up to now, few studies focus on V and Zn co-modified TiO_2 films for degradation of organic pollutants.

In this paper, we adopted a sol–gel process to prepare V and Zn co-doped TiO_2 films on common glass substrates. The photocatalytic activity was evaluated by photodegradation of organic dyes in solution. The mechanism of photoactivity enhancement was also discussed.

2. Experimental

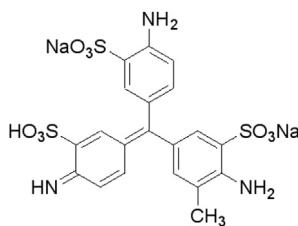
2.1. Preparation of TiO_2 film

All chemicals used in this study were analytical-grade. Deionized water was used throughout in all experiments. TiO_2 film was prepared by the following steps. Firstly, colloidal TiO_2 was prepared by the sol–gel method. Tetra-butyl titanate ($\text{TiO}(\text{C}_4\text{H}_9\text{O})_4$) was added dropwise to ethanol absolute in a clean vessel, and 0.2 M diluted nitric acid was added to the above solution at the speed of 1 drop/sec. under vigorous stirring. The composition of the starting solution was $\text{TiO}(\text{C}_4\text{H}_9\text{O})_4:\text{C}_2\text{H}_5\text{OH}:\text{HNO}_3 = 1:20:20$ in volume ratio. After 48 h aging, the colloidal TiO_2 was obtained. Secondly, we used a controllable dip-coating device to prepare colloidal TiO_2 film on the surface of common glass substrate (25 mm \times 25 mm \times 1 mm) in an ambient atmosphere. The speed withdrawal was controlled at 3 mm s^{-1} . Then, 0.1 mL 5.0×10^{-3} M ammonium metavanadate (NH_4VO_3), 0.1 mL 5.0×10^{-3} M zinc nitrate ($\text{Zn}(\text{NO}_3)_2$), 0.05 mL 1.0×10^{-3} M NH_4VO_3 and 0.05 mL 9.0×10^{-3} M $\text{Zn}(\text{NO}_3)_2$ aqueous solution was doped into the surface layer of TiO_2 gel-film, respectively. Finally, the doped TiO_2 gel-films were calcined in air at 450 $^\circ\text{C}$ for 1 h. In our experiments, the thickness of the film was about 0.6 μm measured using a profilometer

2.2. Characteristic test of TiO_2 film

The identity of crystalline phase was identified by DX-2500 X-ray diffraction (XRD) with a diffractometer employing Cu $\text{K}\alpha$ radiation at a scan rate (2θ) of 0.05 $^\circ\text{S}^{-1}$. Surface morphology of the film was detected using SUPRA 55 high-resolution field emission scanning electron microscopy (FE-SEM). The photoluminescence (PL) emission spectra were recorded at room temperature by a FLS 920 spectrometer with a 300 nm line of 450 W Xenon lamps as excitation source. The emission was scanned in the region of 300–600 nm. The widths of both the excitation slit and the emission slit were set to 3.0 and 2.0 nm, respectively. The Brunauer–Emmett–Teller (BET) surface area of the TiO_2 powders was analyzed by nitrogen adsorption/desorption apparatus (ASAP 2020). UV–vis diffuse reflectance spectra of the film was recorded on a UV–vis spectrophotometer (TU-1901) with an integrating sphere accessory (IS 19-1) using blank glass plate as a reference.

The photocatalytic activity was evaluated by the degradation of acid naphthol red (ANR) dye in aqueous solution under UV-lamp irradiation or visible light irradiation. Structure of acid naphthol red is as following:



Its formula is $\text{C}_{20}\text{H}_{17}\text{N}_3\text{Na}_2\text{O}_9\text{S}_3$, and its maximum of absorption wavelength is about 540 nm. Acid naphthol red is usually used in textile industry due to its good pigmentation. It is well-known that some of dyes are lost during the dyeing process and are released into the environment as textile effluent. Therefore, heightened concerns over public health and associated environmental hazards due to the presence of toxic organic compounds such as dyes in wastewater have been reported.

Ions doped or undoped TiO_2 film was settled in 5 mL acid naphthol red (ANR) aqueous solution with a concentration of 1.0×10^{-4} mol dm^{-3} . A tungsten halogen lamp equipped with UV cut-off filters ($\lambda > 400$ nm) was used as a visible light source whose average light intensity was 40 mW cm^{-2} , and the wavelength of 365 nm was used as a UV light source. UV–vis Spectrometer (TU-1901) was adopted to assess the photodegradation activity of the film photocatalysts. The degradation rate of photocatalysis can be calculated by formula $D = (A_0 - A)/A_0 \times 100\%$, as previously reported [12].

3. Results and discussion

3.1. Microstructures

FE-SEM can be used to examine the surface morphology of the doped or un-doped TiO_2 film. Fig. 1 shows the surface morphology of the un-doped TiO_2 or V/Zn co-doped TiO_2 film calcined at 450 $^\circ\text{C}$ in air for 1.0 h. It is clear that the films are composed of round-like nanoparticles or aggregates. Compared with un-doped TiO_2 film (1a), the surface of V/Zn co-doped TiO_2 film (1b) is relatively uniform and smooth without cracks. It is well-known that a good dispersion or reduced aggregation among particles may increase the active site-reactant contact area, thus enhance photocatalytic degradation of organic dyes. X-ray energy dispersive spectroscopy (EDS) element analyses indicate that the atomic ratio of Ti/O/V/Zn in doped TiO_2 film is 37.62/58.99/1.61/1.86. According to the literature [13,14], chemical states of V and Zn are +5, +4 and +2, 0, respectively. The presence of V^{4+} or Zn^0 in the catalysts may be due to the reduction of V^{5+} or Zn^{+2} by the organics from starting materials.

XRD can be used to investigate the phase structure of the doped and un-doped TiO_2 samples. The XRD patterns of un-

doped TiO_2 and V/Zn co-doped TiO_2 are shown in Fig. 2. It can be seen that after annealing at 450 °C for 1 h, there is a mixed crystallinity constituted of anatase (25.6°, 37.6°, 48.2°), rutile (27.5°, 36.2°), and brookite (30.9°), but the main phase is anatase. What's more, the diffraction peaks of rutile and brookite become weaker after V/Zn codoping. According to the Scherrer formula: $D = 0.89\lambda / \beta \cos \theta$, in which β is the half-height width of the diffraction peak of anatase, θ is the diffraction angle, and λ is the X-ray wavelength which

corresponded to the Cu K α radiation. The average crystallite sizes of the un-doped TiO_2 is 6.9 nm, while V/Zn co-doped TiO_2 samples is 5.4 nm. Both the increase of anatase phases and the decrease of particles size are favorable to photodegradation.

Fig. 3 shows N_2 adsorption/desorption isotherms of the un-doped TiO_2 and V/Zn co-doped TiO_2 powders calcined at 450 °C in air for 1.0 h. BET surface areas can be determined using nitrogen adsorption and desorption isotherms. From

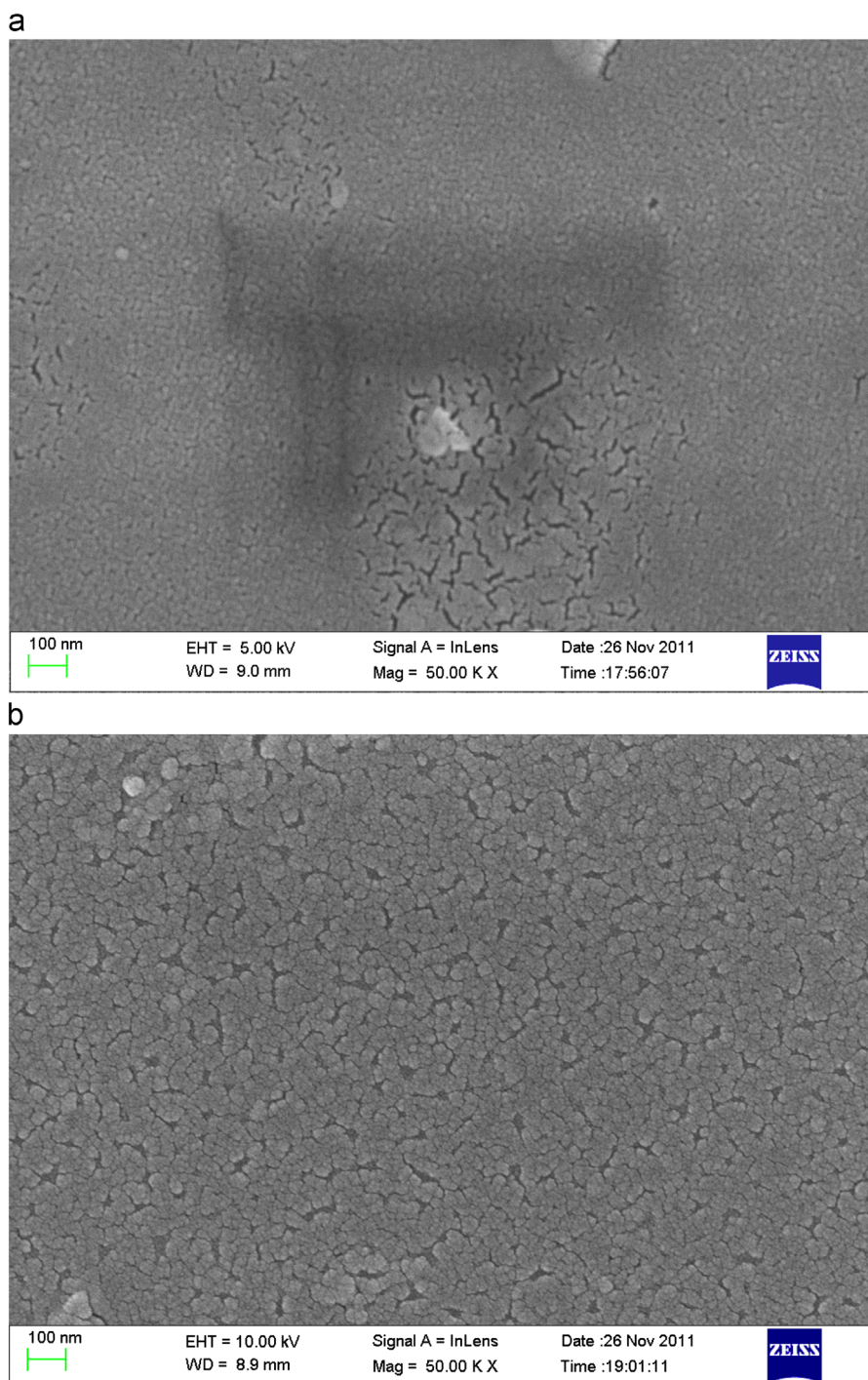


Fig. 1. FE-SEM images of (a) un-doped TiO_2 and (b) V/Zn co-doped TiO_2 films.

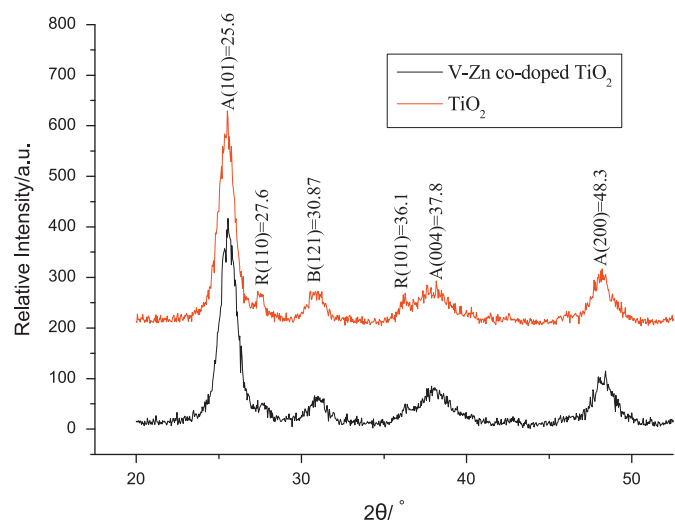


Fig. 2. XRD patterns of un-doped TiO_2 and V/Zn co-doped TiO_2 samples.

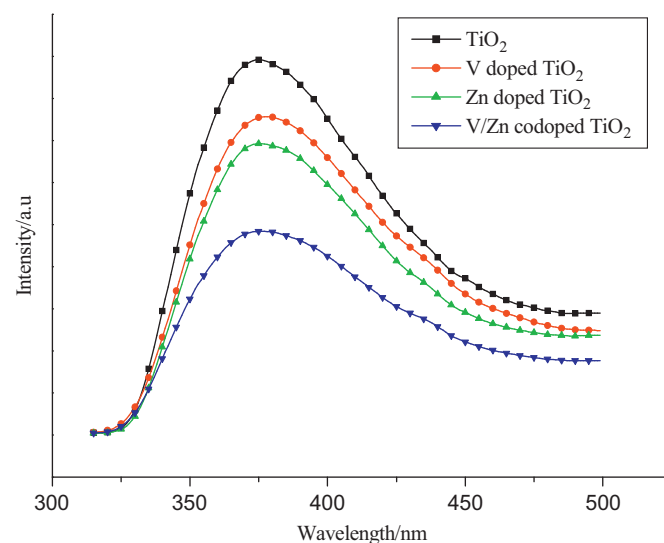


Fig. 4. Photoluminescence spectra of un-doped TiO_2 , single doped and V/Zn co-doped TiO_2 films.

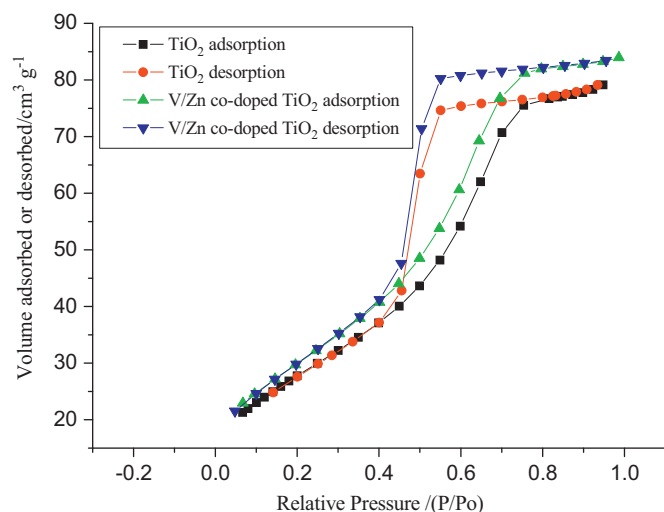


Fig. 3. N_2 adsorption/desorption isotherms of un-doped TiO_2 and V/Zn co-doped TiO_2 samples.

Fig. 3, the isotherms of the two samples exhibit hysteresis loops at high relative pressures from 0.4 to 0.8. It is evident that with the same relative pressure V/Zn co-doped TiO_2 samples have higher adsorption quantities as well as higher surface area. In our case, the specific surface area of un-doped TiO_2 was determined to be $68.40 \text{ m}^2 \text{ g}^{-1}$, while V/Zn co-doped TiO_2 sample is $110.04 \text{ m}^2 \text{ g}^{-1}$. The larger specific surface area is also favorable to the photocatalytic degradation.

Photoluminescence emission is useful to understand the fate of electron–hole pairs in semiconductor particles [15]. The PL emission spectra of four samples in Fig. 4 were examined in the wavelength range of 325–500 nm in our study. It shows that the position of the peaks about 375 nm due to the emission of the band gap transition is similar while PL intensities are different for three samples. The PL

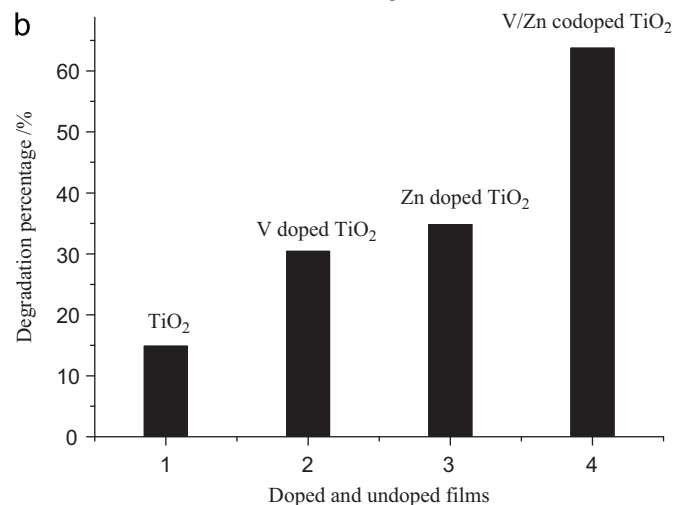
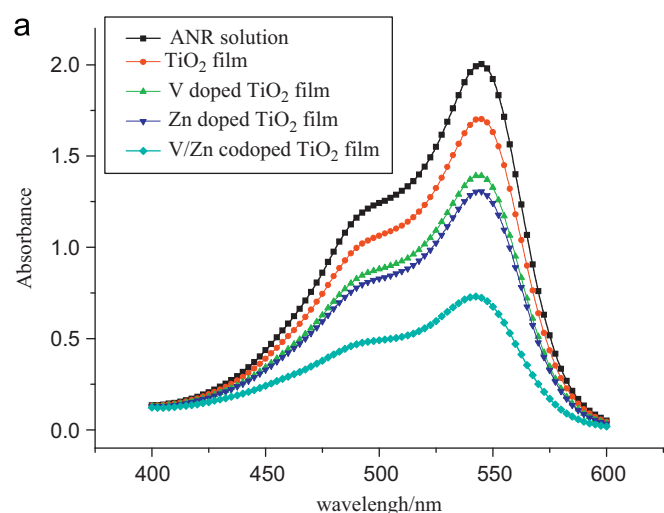


Fig. 5. Absorption spectra (a) and degradation percentage (b) of ANR solutions using a certain amount of V, Zn, V/Zn doped and un-doped TiO_2 films on glass substrates after irradiated for 45 min.

intensity of V/Zn co-doped TiO_2 was the lowest among all samples, indicating the recombination of electron and hole was effectively prohibited compared with un-doped TiO_2 or single doped TiO_2 . Lower recombination of electron and hole can result in higher photocatalytic activity of TiO_2 .

3.2. Photocatalytic activity

Fig. 5 shows UV–Vis absorption spectra (a) and degradation percentage (b) of ANR solutions using an appropriate amount of V, Zn, V/Zn doped and un-doped TiO_2 films on

glass substrates under UV-lamp irradiation with wavelength of 365 nm for 45 min. From Fig. 5b, the degradation percentage of TiO_2 film is 15%; V doped TiO_2 film 30%; Zn doped TiO_2 film 35%; and V/Zn co-doped TiO_2 film 64% in our case. Similarly, the degradation percentage of aqueous ANR using TiO_2 film, V doped TiO_2 film, Zn doped TiO_2 film, and V/Zn co-doped TiO_2 film after visible light irradiated for 45 min is 6%, 12%, 13%, and 20%, respectively. Therefore, we can draw the conclusion that V and Zn co-doped TiO_2 films have the best photocatalytic activity under both UV and visible light irradiation compared with

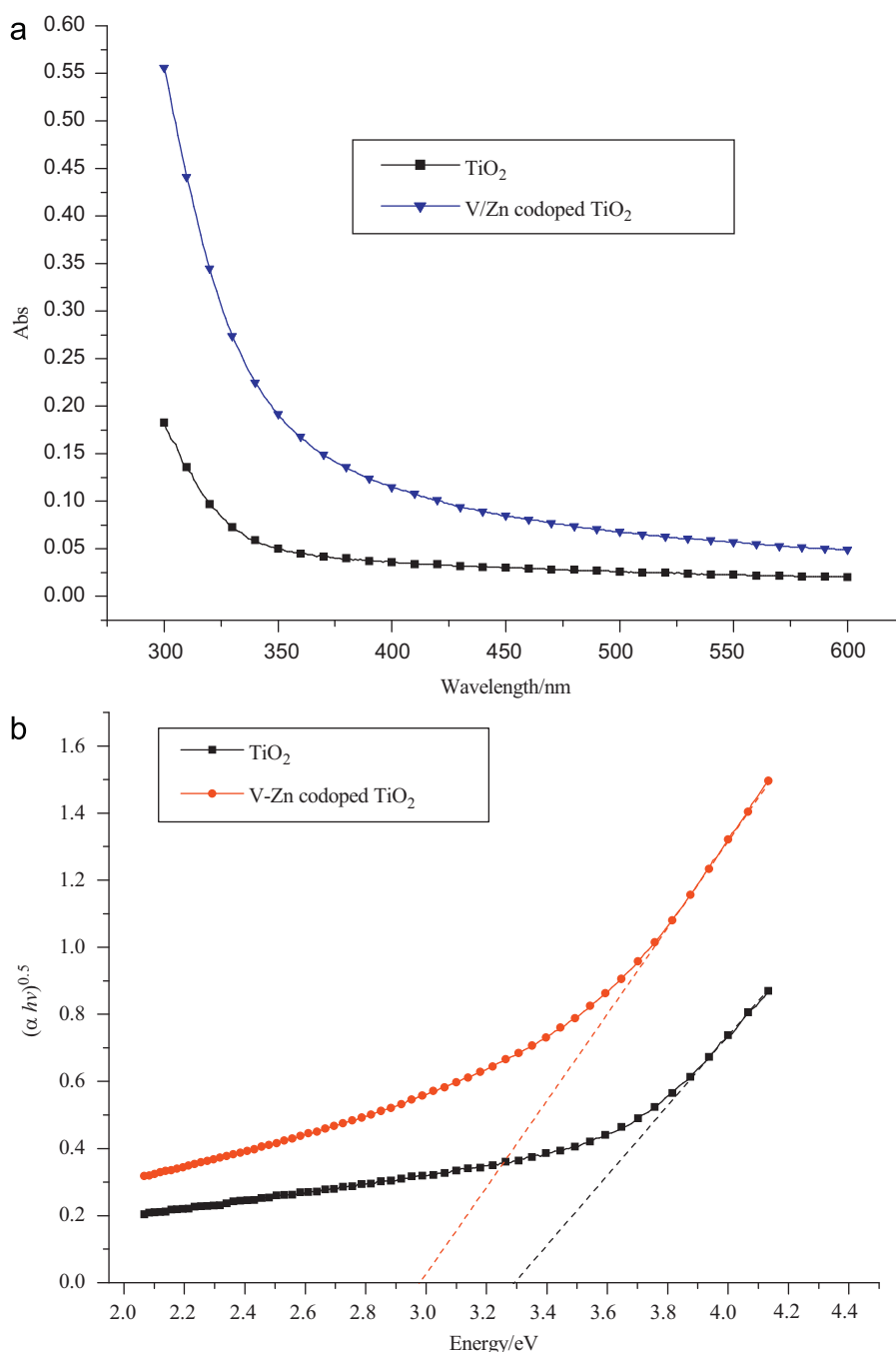


Fig. 6. Diffuse reflection UV–vis absorption spectra (a) and plots of $(\alpha h\nu)^{1/2}$ versus energy ($h\nu$) (b) for un-doped TiO_2 and V/Zn co-doped TiO_2 films.

single doped or un-doped one. It is noted that the degradation percentage of aqueous ANR using un-doped TiO₂ film is also 6% after visible light irradiated for 45 min. This may be related to direct absorption of visible light by the dye, which can lead to charge injection from the excited state of the dye to the conduction band of the semiconductor; resulting in the redox degradation of the organic pollutants [16].

V and Zn codoping can result from formation of multi-dopant energy level within the band gap of TiO₂. Thus, a low concentration codoping can effectively narrow the band gap. These impurities not only serve as trapping centers to retard charge recombination, but also extend the excitation wavelength from the UV to the visible light range. Fig. 6a shows the diffuse reflection UV–vis absorption spectra of un-doped TiO₂ film and V/Zn co-doped TiO₂ film. The absorbance onset of V and Zn co-doped TiO₂ film red shift obviously to more than 450 nm compared with that of undoped TiO₂ film 350 nm. As a result, more photogenerated carriers can join in the degradation reaction; leading to enhance the photocatalytic activity of the V and Zn co-doped TiO₂ film. On the other hand, the optical band gap can be deduced from the equation for a crystalline semiconductor: $\alpha h\nu = A(h\nu - E_g)^{n/2}$, where α , ν , E_g and A are the absorption coefficient, light frequency, band gap, and a constant, respectively [17]. The value of n is determined by the type of optical transition of a semiconductor. Therefore, the band gap energy of TiO₂ can be determined from a plot of $(\alpha h\nu)^{1/2}$ versus energy ($h\nu$), as shown in Fig. 6b. It can be seen that the band gap of V and Zn co-doped TiO₂ film is 2.98 eV compared with that of un-doped TiO₂ film 3.28 eV. The lower band gap has a positive effect on the photocatalytic activity because photocatalytic reactions can be activated by photons with lower energy.

4. Conclusions

Our experimental results confirmed that V and Zn codoping significantly improved the photodegradation of organic dye. The obviously red shift and lower band gap of the modified film may promise a potential application for TiO₂ film in visible light or solar light. In addition, the film may also be potentially used to remove colorless organic pollutants from wastewater.

Acknowledgments

This work was financially supported partially by the National Natural Science Foundation of China (Grant no. 51102114), the Shandong Provincial Natural Science Foundation, China (ZR2012BM009) and the Innovation Foundation of Universities of Ningxia (ZZ201205).

References

- [1] M. Bettinelli, V. Dallacasa, D. Falcomer, P. Fornasiero, V. Gombac, T. Montini, L. Romano, A. Speghini, Photocatalytic activity of TiO₂ doped with boron and vanadium, *Journal of Hazardous Materials* 146 (2007) 529–534.
- [2] A. Eshaghi, R. Mozaffarinia, M. Pakshir, A. Eshaghi, Photocatalytic properties of TiO₂ sol–gel modified nanocomposite films, *Ceramics International* 37 (2011) 327–331.
- [3] C.C. Wu, C.F. Yang, Y.T. Hsieh, W.R. Chen, C.G. Kuo, H.H. Huang, Effects of tungsten thickness and annealing temperature on the electrical properties of W–TiO₂ thin films, *Ceramics International* 38 (2012) 223–227.
- [4] K. Li, Y. He, Y.L. Xu, Y.L. Wang, J.P. Jia, Degradation of rhodamine B using an unconventional graded photoelectrode with wedge structure, *Environmental Science and Technology* 45 (2011) 7401–7407.
- [5] N. Zhao, Y. Yao, J.J. Feng, M.M. Yao, F. Li, Enhanced photocatalytic activity of Co surface doped nanocrystalline TiO₂–SiO₂ composite films, *Water, Air, and Soil Pollution* 223 (2012) 5855–5864.
- [6] Y.Z. Qu, M.M. Yao, F. Li, X.H. Sun, Microstructures and photocatalytic properties of Fe³⁺/Ce³⁺ codoped nanocrystalline TiO₂ films, *Water, Air, and Soil Pollution* 221 (2011) 13–21.
- [7] F. Li, X.L. Yin, M.M. Yao, J. Li, Investigation on F–B–S tri-doped nano-TiO₂ films for the photocatalytic degradation of organic dyes, *Journal of Nanoparticle Research* 13 (2011) 4839–4846.
- [8] S.M. Chang, W.S. Liu, Surface doping is more beneficial than bulk doping to the photocatalytic activity of vanadium-doped TiO₂, *Applied Catalysis B* 101 (2011) 333–342.
- [9] X.C. Lu, J.C. Jiang, K. Sun, D.D. Cui, Characterization and photocatalytic activity of Zn²⁺–TiO₂/AC composite photocatalyst, *Applied Surface Science* 258 (2011) 1656–1661.
- [10] R. Jaiswal, N. Patel, D.C. Kothari, A. Miotello, Improved visible light photocatalytic activity of TiO₂ co-doped with vanadium and nitrogen, *Applied Catalysis B* 126 (2012) 47–54.
- [11] A. Charanpaharia, S.S. Umarea, S.P. Gokhale, V. Sudarsanc, B. Sreedhard, R. Sasikalac, Enhanced photocatalytic activity of multi-doped TiO₂ for the degradation of methyl orange, *Applied Catalysis B* 443–444 (2012) 96–102.
- [12] N. Zhao, M.M. Yao, F. Li, F.P. Lou, Microstructures and photocatalytic properties of Ag⁺ and La³⁺ surface codoped TiO₂ films prepared by sol–gel method, *Journal of Solid State Chemistry* 184 (2011) 2770–2775.
- [13] S. Liu, T.H. Xie, Z. Chen, J.T. Wu, Highly active V–TiO₂ for photocatalytic degradation of methyl orange, *Applied Surface Science* 255 (2009) 8587–8592.
- [14] M. Biesinger, L. Laua, A. Gerson, R. Smart, Resolving surface chemical states in XPS analysis of first row transition metals, oxides and hydroxides: Sc, Ti, V, Cu and Zn, *Applied Surface Science* 257 (2010) 887–898.
- [15] H. Yamashita, M. Harada, J. Misaka, M. Takeuchi, B. Neppolian, M. Anpo, Photocatalytic degradation of organic compounds diluted in water using visible light-responsive metal ion-implanted TiO₂ catalysts: Fe ion-implanted TiO₂, *Catalysis Today* 84 (2003) 191–196.
- [16] C.C. Chen, W.H. Ma, J.C. Zhao, Semiconductormediated photodegradation of pollutants under visible–light irradiation, *Chemical Society Reviews* 39 (2010) 4206–4219.
- [17] X.D. Yan, C.W. Zou, X.D. Gao, W. Gao, ZnO/TiO₂ core–brush nanostructure: processing, microstructure and enhanced photocatalytic activity, *Journal of Materials Chemistry* 22 (2012) 5629–5640.